

# Self-consistent capacitance model for multilayer graphene nanoribbon interconnects

Atul Kumar Nishad, Rohit Sharma

Department of Electrical Engineering, Indian Institute of Technology Ropar, Nangal Road, Rupnagar 140001, India  
E-mail: rohit@iitrpr.ac.in

Published in Micro & Nano Letters; Received on 14th January 2015; Revised on 11th May 2015; Accepted on 11th May 2015

An analytical model for the computation of equivalent capacitance in top-contact and side-contact multilayer graphene nanoribbon interconnects is presented, taking into consideration the interlayer coupling. On the basis of this model, it is observed that interlayer capacitance is a dominant factor that severely degrades the performance of graphene interconnects. The proposed model is verified with simulation data obtained using Synopsys Raphael that exhibits excellent accuracy. Further, a theoretical framework for improvement in key interconnect performance indices such as delay, energy-delay product and bandwidth density is provided by inserting metal atoms between the graphene layers in top-contact graphene nanoribbon interconnects.

**1. Introduction:** Transistors and interconnects both play a crucial role in the performance of microprocessors and other integrated circuits. However, interconnect performance is a major bottleneck in deep submicron technologies, which has resulted in a sustained focus on improving interconnect performance for fast and reliable signal transmission [1]. Currently, copper (Cu) is the industry-preferred interconnect material for on-chip and chip–chip applications [2]. However, below 22 nm technology node, surface and grain boundary scattering increase the resistivity of Cu significantly [3]. Therefore, we need novel interconnect materials to meet the future International Technology Roadmap for Semiconductor (ITRS) requirements. Carbon-based allotropes such as carbon nanotubes (CNTs) and graphene nanoribbons (GNRs) are seen as potential candidates for on-chip interconnects and devices [4, 5] because of their extraordinary electronic and thermal properties. These include larger mean free path, higher thermal conductivity and better current carrying capability [6]. Although CNTs require a complex fabrication process because of their non-planar geometry, patterning of GNR interconnects can be easily achieved using high-resolution lithography [7]. Therefore, GNRs are preferred over CNTs for on-chip interconnect applications. Owing to higher resistance of single-layer GNR, multiple layers of graphene stacked over each other (MLGNRs) are preferred for on-chip interconnects. On the basis of their connection with other devices or interconnects, MLGNRs can be classified as top-contact MLGNRs and side-contact MLGNRs [8]. In case of top-contact MLGNRs (or TC-MLGNRs), only the topmost layer is connected with metallic contacts. On the other hand, all layers are connected to metallic contacts in the case of side-contact MLGNRs (or SC-MLGNRs). It is seen that the fabrication of TC-MLGNNR interconnects is easier than SC-MLGNNR interconnects [9].

Generally, equivalent RLGC-based circuit models are used to compute the performance parameters for TC-MLGNNR interconnects [10], the accuracy of which depends on the correct estimation of line parasitics. In [8, 10, 11], the authors have presented elaborate analytical models for resistance and conductance in TC-MLGNRs. However, an accurate modelling of capacitance for TC-MLGNNR interconnects is equally important. In [10, 12], the authors have obtained the capacitance of TC-MLGNRs by assuming that all GNR layers can be combined to form a single electrode. However, this work ignores the presence of interlayer capacitance between the GNR layers. In TC-MLGNRs, only the topmost layer is coupled to the metallic contacts, resulting in this layer having higher potential than the ones below it. This leads to an interlayer capacitive component in TC-MLGNRs, as shown in

Fig. 1. Note that the interlayer capacitance does not exist in the case of SC-MLGNNR interconnects as all the layers are coupled to the metallic contacts and are equipotential. In [13], the authors have analysed the effect of interlayer capacitance in bilayer graphene. Fig. 2 shows the equivalent capacitance of TC-MLGNNR interconnects with and without the interlayer capacitive component. Equivalent capacitance considering interlayer coupling is computed using Synopsys Raphael [14] and is compared with the previously reported model [10]. From Fig. 2, it is clear that the presence of interlayer capacitance increases the equivalent capacitance by  $2\times$  for both armchair (ac-) and zigzag (zz-) MLGNRs. Thus, the existing capacitance models reported in the available literature fail to capture this effect. The equivalent capacitance directly affects important interconnect performance metrics such as delay, energy and bandwidth budgets. In other words, the previously reported models overestimate the GNR performance as they do not consider this phenomenon. Thus, we need accurate analytical formulation that computes the equivalent capacitance per unit length (p.u.l.) considering interlayer coupling. This is the central theme of our present work.

In this Letter, we propose a rigorous and self-consistent analytical model for capacitance calculation in MLGNNR interconnects, which takes into account interlayer coupling. Our analytical results are compared with simulation data obtained using Synopsys Raphael and exhibit an accuracy within 8%. Next, using our proposed model, we evaluate the effect of interlayer coupling on key performance metrics including delay, energy-delay product (EDP) and bandwidth density (BWD). We observe that interlayer capacitance results in inferior performance of TC-MLGNRs. To improve their performance, we propose improvement in interlayer conductance by introducing metal atoms between the GNR layers [15]. Our analysis shows that the improved TC-MLGNRs with interlayer metal doping can outperform Cu interconnects.

**2. Proposed capacitance model:** In Fig. 1, the interconnect width is  $w$  and thickness is  $t$ . Interlayer distance  $\delta$  is assumed to be 0.35 nm. The dielectric constant between two GNR layers is taken as 1 [16]. Typical interconnect dimensions are obtained from the ITRS [2]. The equivalent capacitance  $C$ , in terms of quantum,  $C_Q$ , and electrostatic capacitances,  $C_E$ , for any MLGNNR interconnect is given by

$$[C] = ([C]_Q^{-1} + [C]_E^{-1})^{-1} \quad (1)$$

The quantum capacitance matrix is a diagonal matrix with diagonal

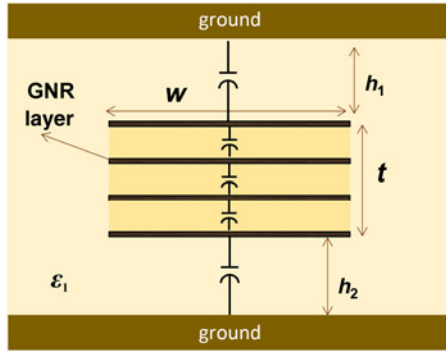


**Figure 1** Schematic of multilayer GNR highlighting interlayer capacitance

elements as  $C_Q$ . For a single-layer GNR,  $C_Q$  is given by

$$C_Q = \frac{4e^2 N_{ch}}{h v_F} \quad (2)$$

Here,  $e$  is the electronic charge,  $h$  the Planck's constant,  $v_F$  the Fermi velocity and  $N_{ch}$  represents the number of conduction channels in GNR [17, 18].

To calculate electrostatic capacitance,  $C_E$ , we need to understand the various capacitive terms originating in an MLGNR interconnect. For an  $N$ -layer MLGNR, the electrostatic capacitance matrix would be of size  $N \times N$ . The top and bottom diagonal elements of the matrix are the sum of the capacitances between top/bottom layer and ground ( $C_{10}$  and  $C_{N0}$ , respectively) and that with their adjacent layers ( $C_{int}$ ). Note that subscript '0' represents ground. The inner diagonal elements represent the capacitance between any GNR layer with its adjacent layers and is given by  $2C_{int}$ . The interlayer layer capacitance between non-adjacent layers would be

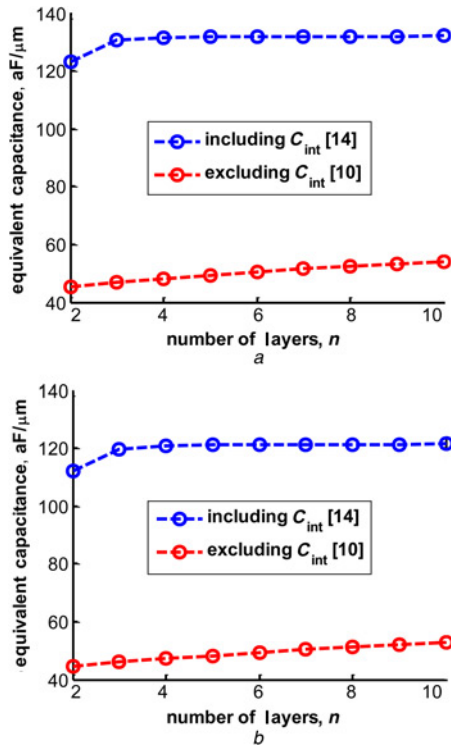


**Figure 2** Equivalent capacitance for zigzag (zz)- and armchair (ac)- TC-MLGNR interconnects  
a zz-TC-MLGNR interconnects  
b ac-TC-MLGNR interconnects

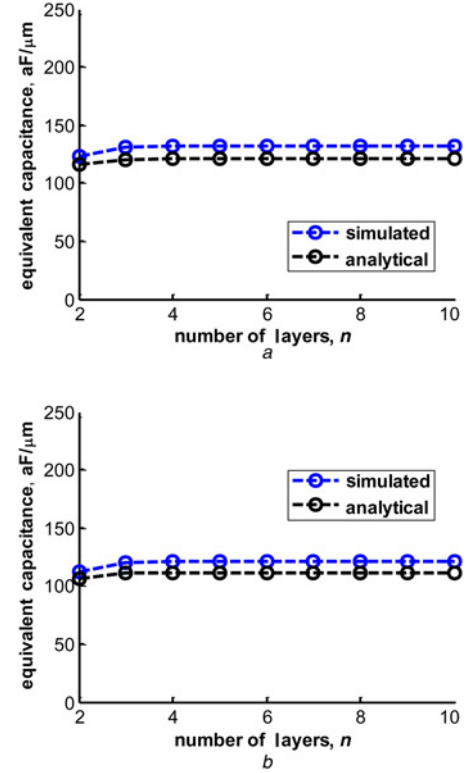


**Figure 3** Comparison between analytical results and simulation data for equivalent capacitance of zz- and ac-type TC-MLGNR interconnects  
a zz-type TC-MLGNR interconnects  
b ac-type TC-MLGNR interconnects

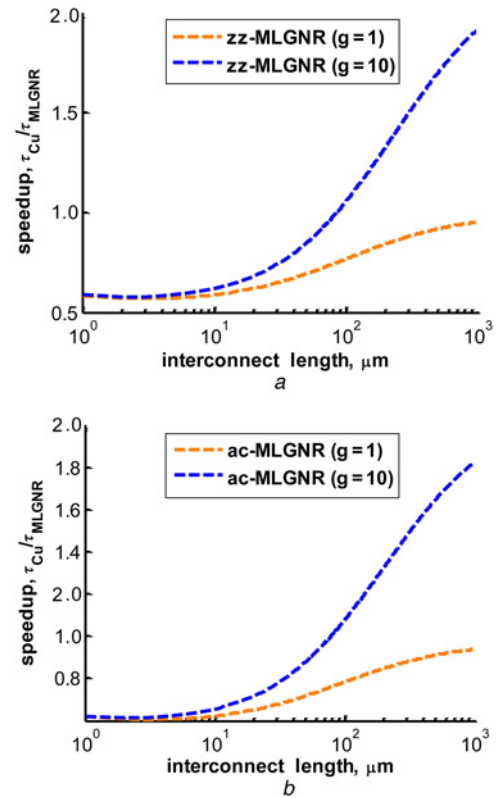


**Figure 4** Speed-up against interconnect length for zz- and ac-type TC-MLGNRs  
a zz-type TC-MLGNRs  
b ac-type TC-MLGNRs

insignificant and is ignored. The electrostatic capacitance  $[C]_E$  matrix can now be computed as (see (3)) where

$$C_{10} = X[w, h_1] \quad (4)$$

$$C_{N0} = X[w, h_2] \quad (5)$$

$$C_{\text{int}} = k_{\text{diel}} \left[ \frac{w}{\delta} + \frac{4 \log(2)}{\pi} \right] \quad (6)$$

Note that  $k_{\text{diel}}$  is the interlayer dielectric constant and is considered to be 1. The function,  $X$ , can be obtained using the conformal mapping method given in [19] as

$$X(a, b) = \varepsilon_1 M \left[ \tanh \left( \frac{\pi a}{4b} \right) \right] \quad (7)$$

where

$$M(\gamma) = \begin{cases} \frac{2\pi}{\ln \left( 2 \left( 1 + \sqrt[4]{1 - \gamma^2} \right) / \left( 1 - \sqrt[4]{1 - \gamma^2} \right) \right)}, & 0 \leq \gamma \leq \frac{1}{\sqrt{2}} \\ \frac{2}{\pi} \ln \frac{2(1 + \sqrt{\gamma})}{1 - \sqrt{\gamma}}, & \frac{1}{\sqrt{2}} \leq \gamma \leq 1 \end{cases} \quad (8)$$

Substituting (2) and (3) in (1), we can now compute the equivalent capacitance for both TC-MLGNRs and SC-MLGNRs. The equivalent capacitance for TC-MLGNRs is given by

$$C_{\text{TC-MLGNR}} = [C]_{N \times N}(1, 1) \quad (9)$$

Here, (1,1) indicates the element of the matrix in the first row and first column. Similarly, the equivalent capacitance for SC-MLGNRs is the summation of all matrix elements and is given by

$$C_{\text{SC-MLGNR}} = \sum \sum [C]_{N \times N} \quad (10)$$

We can now compute equivalent capacitance p.u.l. for MLGNR interconnects considering interlayer coupling. To establish the veracity of our proposed model, we compare the analytical results obtained using (9) with simulation data obtained using Synopsys Raphael. We have verified the model for both ac- and zz- configurations of TC-MLGNRs. As shown in Figs. 3a and b, our analytical results exhibit an accuracy within 8% for both configurations with lesser computational effort.

For performance analysis of TC-MLGNRs, we have considered ITRS year 2024 technology nodes [2]. In that, the interconnect width  $w$ ; the distance between the first layer and ground,  $h_1$ ; the distance between  $N$ th layer and ground,  $h_2$ ; and the surrounding dielectric constant  $\varepsilon_1$  are 7.5 nm, 15 nm, 15 nm and 1.99, respectively. In our analysis, interconnect delay is computed using the standard expression given in [20] and is directly proportional to equivalent

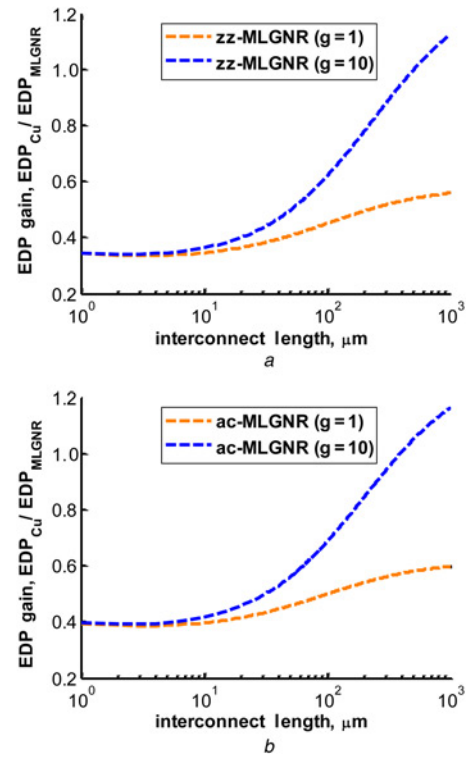


**Figure 5** EDP gain against interconnect length for zz- and ac-type TC-MLGNRs

a zz-type TC-MLGNRs

b ac-type TC-MLGNRs

capacitance. As mentioned earlier, previously reported models [10] give an optimistic estimation of GNR interconnect performance, when compared with Cu interconnects. However, once interlayer capacitance is taken into account, our analytical results suggest that TC-MLGNRs exhibit inferior performance as compared with Cu interconnects. One possible way to improve the performance of TC-MLGNR interconnects is by increasing their interlayer conductance. Introducing metal atoms between GNR layers can improve interlayer conductance [8]. For longer interconnect lengths, significant improvement in delay in TC-MLGNR interconnects is seen when the interlayer conductance is increased by  $10\times$  ( $g=10$ ), as shown in Fig. 4. In Fig. 4, delay ratio between Cu and TC-MLGNR interconnects, or speed-up, as a function of interconnect length is presented for both ac- and zz-type TC-MLGNRs. Although undoped TC-MLGNR interconnects show inferior performance to Cu, significant speed-up (by  $2\times$ ) can be achieved using interlayer metal doping.

In Fig. 5, the improvement in EDP ratio between Cu and TC-MLGNR interconnects, or EDP gain, as a function of interconnect length for zz- and ac-type TC-MLGNR interconnects is shown. Our results show that interlayer capacitance degrades the EDP of TC-MLGNR interconnects. However, the optimised TC-MLGNR interconnects (with  $g=10$ ) can offer higher EDP as compared

$$[C]_E = \begin{bmatrix} C_{10} + C_{\text{int}} & -C_{\text{int}} & 0 & 0 & 0 & 0 & 0 & 0 \\ -C_{\text{int}} & 2C_{\text{int}} & -C_{\text{int}} & 0 & 0 & 0 & 0 & 0 \\ 0 & -C_{\text{int}} & 2C_{\text{int}} & -C_{\text{int}} & 0 & 0 & 0 & 0 \\ \vdots & 0 & \ddots & \ddots & \ddots & 0 & \vdots & \vdots \\ \vdots & \vdots & 0 & \ddots & \ddots & \ddots & 0 & \vdots \\ 0 & 0 & 0 & 0 & -C_{\text{int}} & 2C_{\text{int}} & -C_{\text{int}} & 0 \\ 0 & 0 & 0 & 0 & 0 & -C_{\text{int}} & 2C_{\text{int}} & -C_{\text{int}} \\ 0 & 0 & 0 & 0 & 0 & 0 & -C_{\text{int}} & C_{\text{int}} + C_{N0} \end{bmatrix}_{N \times N} \quad (3)$$

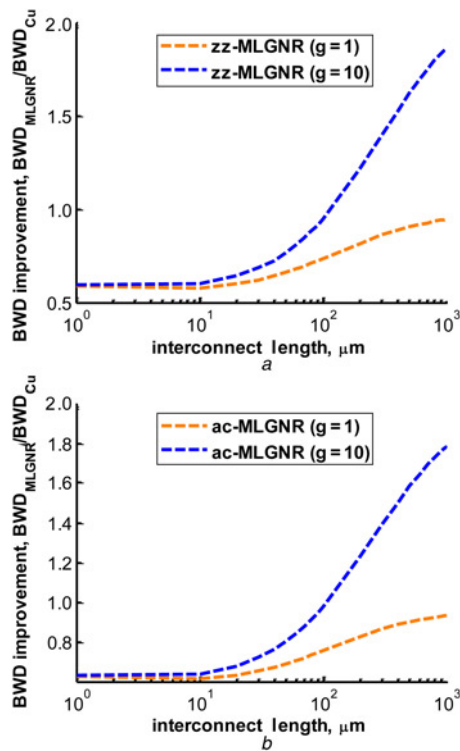


**Figure 6**  
a Improvement in BWD in the case of zz-type TC-MLGNRs  
b Improvement in BWD in the case of ac-type TC-MLGNRs

with Cu interconnects. The EDP gain improves by  $2\times$  for TC-MLGNRs with interlayer metal doping when compared with undoped TC-MLGNRs.

Finally, improvement in BWD for TC-MLGNRs over Cu interconnects is shown in Fig. 6. Again, unlike previously reported data, we see that BWD of TC-MLGNRs is lower than Cu interconnects because of interlayer capacitance. However, by improving interlayer conductance ( $g = 10$ ), one can expect BWD of our optimised TC-MLGNRs to be significantly higher (by  $1.8\times$ ) than that of Cu interconnects.

**3. Conclusions:** The authors feel that interlayer capacitance is a significant contributor to overall capacitance in TC-MLGNRs and needs to be considered in computing equivalent line capacitance. To that end, we present an analytical model that computes the equivalent capacitance p.u.l. considering interlayer coupling. The model is verified using exhaustive simulation data and is valid for both TC- and SC-MLGNRs. To highlight the importance of our study, we present elaborate performance analysis of TC-MLGNRs using our proposed model. We observe that interlayer coupling results in overall inferior performance of TC-MLGNRs when compared with Cu interconnects. Performance improvement can be achieved by improving its interlayer conductance using metal doping between adjacent GNR layers. These optimum TC-MLGNR interconnects with doped

metal atoms can significantly exceed the performance of Cu interconnects and are seen as potential candidates for future interconnect and device applications.

#### 4 References

- [1] Ceyhan A., Naeemi A.: 'Cu interconnect limitations and opportunities for SWNT interconnects at the end of the roadmap', *IEEE Trans. Electron Devices*, 2013, **60**, (1), pp. 374–382
- [2] Semiconductors, I.T.R.S., 2011
- [3] Steinhogel W.: 'Comprehensive study of the resistivity of copper wires with lateral dimensions of 100 nm and smaller', *J. Appl. Phys.*, 2005, **97**, (2), pp. 023706-1–023706-7
- [4] Kumar P., Singh A., Garg A., Sharma R.: 'Compact models for transient analysis of single-layer graphene nanoribbon interconnects'. IEEE Int. Conf. on Computer Modelling and Simulation (UKSim), 2013, pp. 809–814
- [5] Nishad A.K., Dalakoti A., Jindal A., Kumar R., Kumar S., Sharma R.: 'Analytical model for inverter design using floating gate graphene field effect transistors'. IEEE Computer Society Annual Symp. on VLSI (ISVLSI), 2014, pp. 148–153
- [6] Geim A.K., Novoselov K.S.: 'The rise of graphene', *Nat. Mater.*, 2007, **6**, (3), pp. 183–191
- [7] Berger C., Song Z., Li X., *ET AL.*: 'Electronic confinement and coherence in patterned epitaxial graphene', *Science*, 2006, **312**, (5777), pp. 1191–1196
- [8] Nishad A.K., Sharma R.: 'Analytical time-domain models for performance optimization of multilayer GNR interconnects', *IEEE J. Sel. Top. Quantum Electron.*, 2014, **20**, (1), pp. 3700108-1–3700108-8
- [9] Sui Y., Appenzeller J.: 'Screening and interlayer coupling in multilayer graphene field-effect transistors', *Nano Lett.*, 2009, **9**, (8), pp. 2973–2977
- [10] Kumar V., Rakheja S., Naeemi A.: 'Performance and energy-per-bit modeling of multilayer graphene nanoribbon conductors', *IEEE Trans. Electron Devices*, 2012, **59**, (10), pp. 2753–2761
- [11] Zhao W.S., Yin W.Y.: 'Comparative study on multilayer graphene nanoribbon (MLGNR) interconnects', *IEEE Trans. Electromagn. Compat.*, 2014, **56**, (3), pp. 638–645
- [12] Kumar V., Rakheja S., Naeemi A.: 'Review of multi-layer graphene nanoribbons for on-chip interconnect applications'. IEEE Int. Symp. on Electromagnetic Compatibility (EMC), 2013, pp. 528–533
- [13] Young A.F., Levitov L.S.: 'Capacitance of graphene bilayer as a probe of layer-specific properties', *Phys. Rev. B*, 2011, **84**, (8), p. 085441
- [14] Raphael, <https://www.synopsys.com/tools/tcad/interconnectsimulation/pages/raphael.aspx>
- [15] Weller T.E., Euerby M., Saxena S., *ET AL.*: 'Superconductivity in the intercalated graphite compounds C6Yb and C6Ca', *Nat. Phys.*, 2005, **1**, (1), pp. 39–41
- [16] McCann E.: 'Asymmetry gap in the electronic band structure of bilayer graphene', *Phys. Rev. B*, 2006, **74**, (16), p. 161403
- [17] Naeemi A., Meindl J.D.: 'Compact physics-based circuit models for graphene nanoribbon interconnects', *IEEE Trans. Electron Devices*, 2009, **56**, (9), pp. 1822–1833
- [18] Farshi M.K., Nasiri S.H., Faez R.: 'Compact formulae for number of conduction channels in various types of graphene nanoribbons at various temperatures', *Mod. Phys. Lett. B*, 2012, **26**, (01), p. 1150004
- [19] Stellari F., Lacaita A.L.: 'New formulas of interconnect capacitances based on results of conformal mapping method', *IEEE Trans. Electron Devices*, 2000, **47**, (1), pp. 222–231
- [20] Venkatesan R., Davis J.A., Meindl J.D.: 'Compact distributed RLC interconnect models – part IV: unified models for time delay, crosstalk, and repeater insertion', *IEEE Trans. Electron Devices*, 2003, **50**, (4), pp. 1094–1102